Electrochimica Acta 56 (2011) 9568–9574

Contents lists available at ScienceDirect

Electrochimica Acta

journal homepage: www.elsevier.com/locate/electacta

Progress in the understanding of surface structure and surfactant influence on the electrocatalytic activity of gold nanoparticles

V.C. Ferreira[a,b], J. Solla-Gullón[c], A. Aldaz[c,1], F. Silva[b,1], L.M. Abrantes[a,*,1]

[a] CQB, Departamento de Química e Bioquímica, Faculdade de Ciências da Universidade de Lisboa, Campo Grande, 1749-016 Lisboa, Portugal
[b] CIQ-UP, Linha 4, Departamento de Química, Faculdade de Ciências da Universidade do Porto, Rua do Campo Alegre 687, 4169-007 Porto, Portugal
[c] Instituto Universitario de Electroquímica, Universidad de Alicante, Apartado 99, 03080 Alicante, Spain

ARTICLE INFO

Article history:
Received 9 November 2010
Received in revised form 26 January 2011
Accepted 29 January 2011
Available online 2 March 2011

Keywords:
Gold nanoparticles
Crystallographic orientation
CTAB
Electrocatalytic activity

ABSTRACT

The preparation of gold nanoparticles (Au-NPs) displaying specific shape, size and surface crystallographic domains has been investigated aiming to clarify the effect of the surface crystallographic orientation, of the synthesised nanoparticles, and surfactant influence on the electrochemical response of the ITO/Au-NPs modified electrodes. Polymorphic and nanorod-shaped Au-NPs have been obtained using distinct synthetic procedures in the presence of cetyltrimethylammonium bromide (CTAB), through seed-mediated growth methods, displaying distinct surface crystallographic domains confirmed by transmission electron microscopy, X-ray diffraction analysis and under potential deposition (UPD) of lead.

The nanoparticles have been physically immobilised by casting on indium tin oxide (ITO) surfaces and the electrocatalytic activity of the Au-NPs evaluated using the ascorbic acid (AA) oxidation reaction, by cyclic voltammetry. The polymorphic and distinct surface crystallographic orientations of the Au-NPs were reflected in an irreproducible electrochemical response. Using gold nanorods comprising (1 1 1) and (1 1 0) facets and gold nanocubes consisting of faces displaying (1 0 0) surface domains, by contrasting the behaviour of CTAB-stabilised and clean particles, it has been possible to verify that the distinct voltammetric results are due to the exposure of specific crystallographic orientations owing to dissimilar interaction strength of CTAB with those facets.

1. Introduction

The synthesis of gold nanoparticles (Au-NPs), by wet chemical processes, has been extensively investigated in the last decades aiming to control the size, shape and surface crystallographic orientation of the prepared NPs. The preparation has been achieved, namely by controlling the reactants and seeds concentrations ratio [1], addition of other compounds (e.g. poly(vinyl-pyrrolidone) and silver ions [1–4]), using different reducing agents (e.g. salicylic acid [5]) and several synthetic methodologies, such as the colloidal, seed-mediated and micro-emulsion growth methods [4,6–9]. The possibility of controlling the surface crystallographic orientation of nanoparticles, particularly of gold and platinum, has been investigated envisaging the application of such materials on structure sensitive or site demanding electrocatalytic reactions [4,6–11].

The use of surface-sensitive reactions, such as lead under potential deposition (UPD) on gold [4,7,9,10], irreversible adsorption of adatoms (e.g. Ge or Bi) and methanol, ammonia or formic acid oxidation on platinum [6,7,11], is a useful tool for the characterisation of the surface structure of electrodes. Such reactions can also be employed in the characterisation of nanoparticles surface, without loss of the preferential crystallographic orientation. Lead UPD has been applied for the characterisation of Au-NPs surface crystallographic facets, with the advantage of allowing, at high potential values (above 1 V), the removal of surface contaminants.

Within the seed-mediated growth methods, cetyltrimethylammonium bromide (CTAB) has been the most commonly employed capping agent. It is a cationic surfactant, conferring a positive charge to the nanoparticles and it is known as a structure-directing molecule that interacts differently with the gold facets in the order (1 0 0)≈(1 1 0)>(1 1 1) [12,13] enabling to prepare particles with specific shape and surface crystallographic orientation. However, the presence of surfactants may affect the electrochemical response of surfaces, as observed on carbon electrodes in the presence of ascorbic acid (AA) and dopamine (DA) [14,15]. In fact, with CTAB or didodecyl-dimethylammonium bromide (DDAB), it was possible to discriminate the oxidation peaks of both electroactive species; the AA and DA oxidation peaks potentials appear shifted to lower

* Corresponding author at: CQB, Departamento de Química e Bioquímica, Faculdade de Ciências da Universidade de Lisboa, Campo Grande, 1749-016 Lisboa, Portugal. Tel.: +351 21750000; fax: +351 21750088.
E-mail address: luisa.abrantes@fc.ul.pt (L.M. Abrantes).
[1] ISE Member.

0013-4686/$ – see front matter © 2011 Elsevier Ltd. All rights reserved.
doi:10.1016/j.electacta.2011.01.105

and higher potential values, respectively, when compared with the absence of the surfactants, due to the electrostatic interactions between the positively charged surfactant and DA (repulsive) and anionic AA species (attractive).

Due to the well known electrocatalytic and optical properties of Au-NPs, these have been used for surface modification and its attachment to electrodes has been achieved for instance by self-assembling (e.g. on 3-mercaptopropyltrimethoxysilane (MPTMS) modified indium tin oxide (ITO) surfaces, alkanedithiol SAMs on gold and sulphur containing conducting polymer films), taking advantage from the Au–S interaction [16–19], seed-mediated methods (on ITO surfaces, similarly to the wet chemical synthesis of Au-NPs [16,20]) and casting (on glassy carbon or ITO [3,4,7]). The remarkable electrocatalytic activity of Au-NPs has been investigated [3,18–20]. Spherical Au-NPs (5 or 15 nm) attached to a poly(3-methylthiophene) film, displayed electrocatalytic activity towards the hydrazine oxidation reaction, when compared with the pristine polymer; an improvement on the electrocatalytic performance of the so modified electrodes was achieved by using small size Au-NPs [18]. Au-NPs attached to glassy carbon (GC) surfaces, modified with cysteamine, through Au–S interaction exhibit good electrochemical behaviour and enabled the selective detection of AA and DA [19]. The surface crystallographic orientation of Au-NPs also plays an important rule on the electrocatalytic behaviour of such materials. ITO surfaces modified with Au-NPs displayed distinct electrochemical response towards surface sensitive reactions; gold nanobelts comprising (1 1 0) surface domains present enhanced electrocatalytic behaviour towards the glucose oxidation reaction while the gold plates comprising (1 1 1) facets have a better performance for the methanol oxidation reaction [3] and enable the discrimination of AA and DA oxidation processes [20] similarly to the behaviour of carbon electrodes in the presence of surfactants [14,15]. A sol–gel silicate network modified surface including spherical Au-NPs (70–100 nm), comprising predominantly (1 1 1) surface facets, showed morphology dependent electrocatalytic activity towards AA oxidation reaction and two anodic processes have been detected [21].

In the present work, the synthesis of Au-NPs, displaying controlled shape, size and surface structure, was pursued in order to evaluate their electrocatalytic properties and to investigate how the interaction strength of CTAB with gold facets enable the selective crystallographic orientation exposure of the less stabilised (1 1 1) facets and therefore modulate their electrochemical response.

2. Experimental

2.1. Synthesis and characterisation of Au-NPs

Tetrachloroauric(III) acid ($HAuCl_4$, Alfa Aesar 99, 99%), sodium citrate dihydrate (Alfa Aesar 99%), CTAB (Sigma Ultra 99%), sodium borohydride ($NaBH_4$, Sigma 99%), silver nitrate ($AgNO_3$, Merck p.a.), L(+)-ascorbic acid (AA, Aldrich 99%) and sodium hydroxide (NaOH, Merck p.a.) were used throughout the work.

Gold particles of samples A, B and C, were prepared through seed-mediated growth methods using 3 distinct procedures A, B and C, respectively, which have been previously described in the literature [22–24].

The resulting colloidal suspensions were kept at 25 °C overnight; excess CTAB was removed by centrifugation, washed and re-suspended in ultra-pure water. The Au-NPs from sample A have been purified by removal of the CTAB capping agent and the resulting "surfactant-free" Au-NPs, or cleaned sample A, designated as sample A′; NaOH was added to the colloidal suspension and the resulting precipitate was washed and re-dispersed in ultra-pure water.

The Au-NPs were characterised by UV–vis spectrophotometry (UV-vis, Jasco V560 spectrophotometer), transmission electron microscopy (TEM, Hitachi H-8100 transmission electron microscope, operating at 10–15 kV) and X-ray diffraction analysis (XRD, Philips – PW 1710 diffractometer with Cu Kα radiation (λ = 0.15418 nm) operated at 40 kV and 30 mA with a time per step of 5.000 s and step size of 0.005°).

2.2. Preparation and characterisation of the Au-NPs modified surfaces

The ITO substrates have been cleaned by successive immersion in acetone, ethanol and ultra-pure water, in an ultra-sound bath for 10 min each and the GC surface renewed by hand-polishing in alumina (0.05 μm) and rinsed with ultra-pure water. The Au-NPs were immobilised on the ITO or GC surfaces by drop-casting of 100 μL aliquots on ITO (c.a. 0.9 cm^2 exposed surface area) or c.a. 10 μL on GC (3 mm diameter), under a nitrogen or argon flow, after which the Au-NPs modified substrates were washed with ultra-pure water and dried.

The ITO/Au-NPs surfaces have been characterised by UV–vis, XRD (under the above mentioned conditions) and scanning electron microscopy (FEG-SEM, Field Emission Gun – scanning electron microscope, JEOL 7001F, operating at 10–15 kV).

L(+)-Ascorbic acid 0.5 mmol dm^{-3} in phosphate buffer (PB) solution, pH 7, prepared from sodium dihydrogen phosphate monohydrate, $NaH_2PO_4{\cdot}H_2O$ (Merck, p.a., 99%) and di-sodium hydrogen phosphate anhydrous, Na_2HPO_4 (Merck, p.a., 99%), and $Pb(NO_3)_2$ 1 mmol dm^{-3} (Sigma, 99%) in NaOH 0.1 mol dm^{-3} (Merck, p.a.) solution were employed to characterize by cyclic voltammetry the electrochemical behaviour of the Au-NPs. The lead UPD was performed on the GC/Au-NPs modified electrodes as described in reference [22]. Ultra-pure water was used for the preparation of aqueous solutions.

The electrochemical characterisation was performed in a three compartment cell, using a Pt foil or Au wire and a saturated calomel (SCE) or hydrogen electrode (RHE) as counter and reference electrodes, respectively. The electrochemical experiments have been performed in an IMT Electrochemical Interface and a DEA332 Digital Electrochemical Analyser or a PGSTAT30 AutoLab system. Prior to the measurements, the solutions were de-aerated by bubbling N_2 or argon (high purity, dried) for c.a. 20 min.

3. Results and discussion

3.1. Au-NPs characterisation

The microscopic characterisation of the prepared Au-NPs showed that by the rigorous control of the synthesis conditions, it was possible to prepare gold nanoparticles with specific size and shape, as illustrated in the representative TEM images in Fig. 1. In sample A, rod shaped Au-NPs with average size of 41 per 10 nm, illustrated in the size distribution histogram obtained from more than 300 particles (in c.a. 20 TEM images from each sample), were obtained (Fig. 1a); other samples prepared under the same synthesis conditions yield similar results. Samples B and C resulted in mixed shape and size particles with average size of the spheroid particles of 40 and 80 nm, Fig. 1b and c, respectively.

The spectrophotometric characterisation revealed the presence of two absorption peaks, which correspond to the transversal (at 518 nm) and longitudinal (652 nm) surface plasmon bands [25] of the rod-shaped Au-NPs of sample A (Fig. 2a). After removal of the capping agent, in sample A′, the nanoparticles aggregation was identified in the corresponding UV–vis spectrum by the absorption band broadening at c.a. 665 nm and its shift to higher wavelength

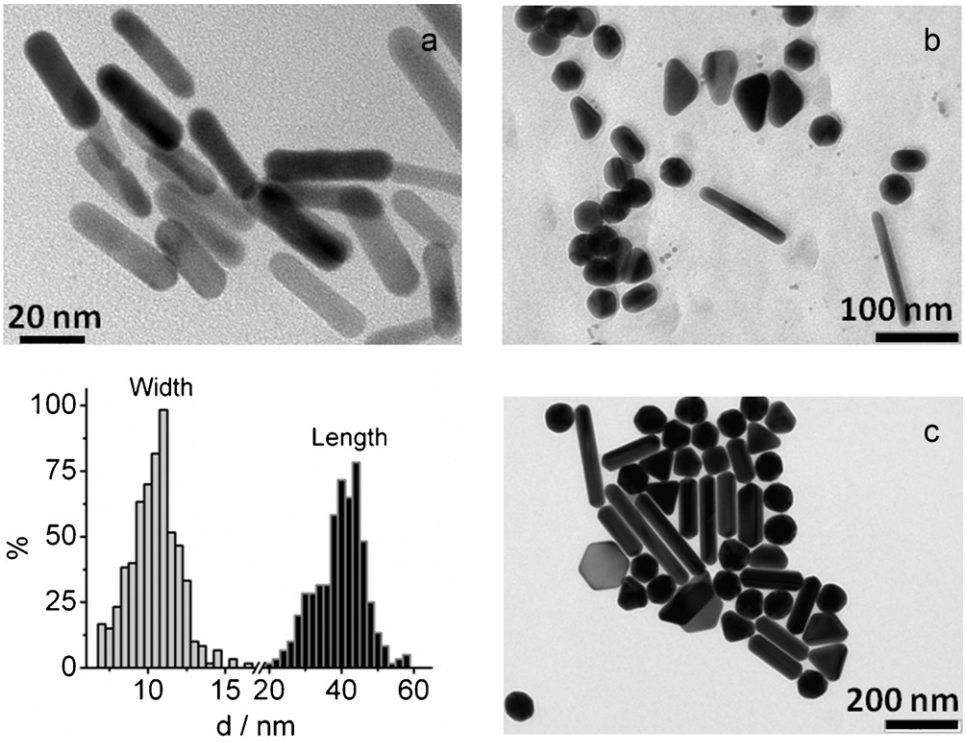

Fig. 1. Representative TEM micrographs of Au-NPs from samples A, B and C with average size of the rod-shaped particles (a) length: 10 ± 2 nm and width: 41 ± 7 nm and corresponding size distribution histogram of Au-NPs in sample A, and of the spheroid particles of samples (b) 38 ± 2 nm and (c) 82 ± 4 nm.

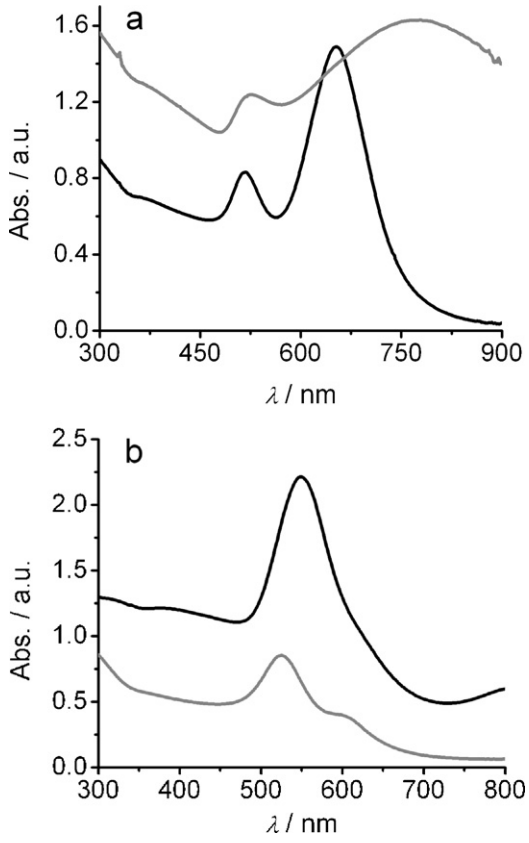

Fig. 2. UV–vis spectra of the Au-NPs from (a) sample A, (—) colloid and (—) "surfactant-free" and (b) sample B (—) and sample C (—).

values (Fig. 2a), in a behaviour similar to that reported for colloidal suspensions of Au-NPs after salt addition [26]. The detection of broad and multiple absorption bands in the UV–vis spectra of samples B and C (Fig. 2b) is due to the presence non-homogeneously sized products, in agreement with the TEM images (Fig. 1b and c).

It is well known that gold nanorods can present (1 1 0) or (1 0 0) side faces and (1 1 1) end faces [7,13,22,27]. Surface-sensitive reactions are well characterised on low index single crystals of gold; for instance, lead under potential deposition presents distinct voltammetric profiles, depending on the specific interactions between the surface atoms of the supporting metal and the depositing atoms of the foreign metal and thus it has been successfully employed in the characterisation of the surface crystallographic orientation of gold nanoparticles without loss of the crystalline surface structure [9,10,22]. Also, the deposition of a film of PbO_2 in basic medium

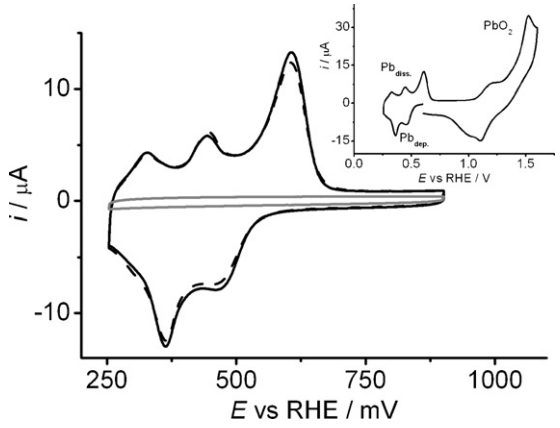

Fig. 3. Voltammetric profiles of the lead UPD on Au-NPs from sample A′ (- - -) before and (—) after PbO_2 deposition/dissolution cycle (inset), in 1 mmol dm^{-3} $Pb(NO_3)_2$ in 0.1 mol dm^{-3} NaOH solution; $\nu = 50$ mV s^{-1}.

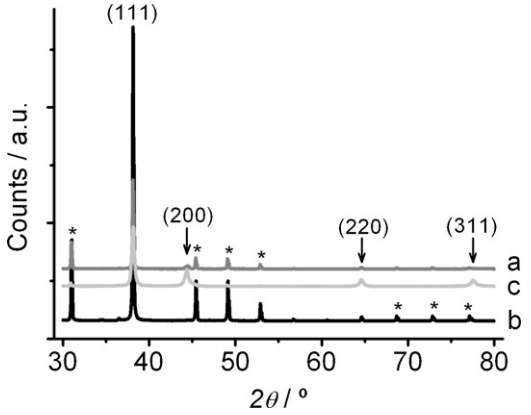

Fig. 4. X-ray patterns of Au-NPs from (a) sample A, (b) sample B and (c) sample C, deposited on amorphous silicon; diffraction lines from the reaction mixture marked with asterisk.

may contribute to the removal of impurities from the gold surface [10], but it is necessary to ensure that the cleaning procedure do not affects the crystallographic surface domains of the particles. Since the PbO_2 deposition occurs at potential values below 1.10 V, it may protect the gold surface of further oxidation at higher potentials. In Fig. 3 are represented the lead UPD voltammetric profiles obtained for Au-NPs from sample A′, immobilised on GC surfaces, before and after the PbO_2 deposition/dissolution cycle (inset in Fig. 3). The slight increase in the lead deposition and dissolution peaks current (Fig. 3), after the lead oxide film deposition and dissolution, showed that a small amount of surface contaminants has been removed from the Au-NPs surface. The lead dissolution peaks detected at about 330, 440 and ~600 mV (vs RHE) in the representative voltammogram obtained for the rod shaped Au-NPs in different samples, Fig. 3, could be assigned to the presence of (1 1 1) and (1 1 0) surface domains in the rod shaped nanoparticles [9,10], in agreement with the literature data for short gold nanorods prepared under the same experimental conditions [22].

All the samples have been subjected to X-ray diffraction analysis and the diffraction peaks detected at 38.11, 44.36, 64.54 and 77.54°, Fig. 4, correspond to the (1 1 1), (2 0 0), (2 2 0) and (3 1 1) facets, related to the fcc crystalline structure of gold (JCPDS file no. 4-0784) revealing that the synthesised gold nanoparticles are crystalline in nature. It is worth noting that the average surface of the Au-NPs from the samples A and B present a higher contribution from the (1 1 1) facet.

3.2. Characterisation of the ITO/Au-NPs modified surfaces

The UV–vis spectra of the Au-NPs immobilised on ITO (Fig. 5a) reveal the typical surface plasmon bands of the Au-NPs, confirming its confinement to the ITO surface. However, it should be pointed out the slight red-shift of the absorption bands which shall be related to the inter-particles coupling due to decreased particles distance [28,29]. SEM imaging corroborates the successful confinement of the nanoparticles on the ITO, Fig. 5b. In the case of sample A′ aggregates have been detected deposited on the top of the ITO surface (Fig. 5b), which also supports the UV–vis data. Dispersed Au-NPs were obtained for samples A and B whereas a higher amount of immobilised nanoparticles is achieved with sample C; the broad range of sizes and shapes of the samples B and C is clearly noticed in the corresponding modified electrodes images (Fig. 5b).

3.3. Electrochemical behaviour of Au-NPs

The electrochemical behaviour of the synthesised Au-NPs has been investigated using the surface sensitive AA oxidation reaction. In neutral medium, the AA is in the deprotonated state ($pK_a = 4.17$) as ascorbate anion (HA^-). It is well accepted [21,30–32] that the AA (or HA^-) oxidation occurs in two oxidation steps according to:

$$AA \leftrightarrow HA^- + H^+ \quad (1)$$

$$HA^- \rightarrow DHA + H^+ + 2e^- \text{ (oxidation I)} \quad (2)$$

$$DHA + H_2O \rightarrow HDHA \quad (3)$$

$$HDHA \rightarrow DKG \text{ (hydrolysis)} \quad (4)$$

$$DKG \rightarrow Prod. + ne^- \text{ (oxidation II)} \quad (5)$$

On gold single-crystal surfaces, the rate determining process (oxidation I) has been referred as insensitive to the gold surface crystallographic orientation and assigned to the oxidation of the AA (or HA^-) to dehydro-L-ascorbic acid (DHA) and/or its hydration products (HDHA), in a complex process involving 2 electrons (Eqs. (2) and (3)) [30–32]. The oxidation product is unstable in aqueous medium and pH > 5 and spontaneous irreversible hydrolysis occurs, Eq. (4), with the lactone ring opening and consequent formation of the 2,3-diketogluconic acid (DKG) [21]. Oxidation II (Eq. (5)) has been considered as sensitive to the surface crystallographic orientation of the gold electrode and assigned to the oxidation of the products resulting from the first oxidation step [21,30].

On clean gold electrodes, distinct voltammetric profiles are obtained as illustrated in Fig. 6; on polycrystalline gold, a single oxidation peak is detected at about 315 mV (Fig. 6a) while on

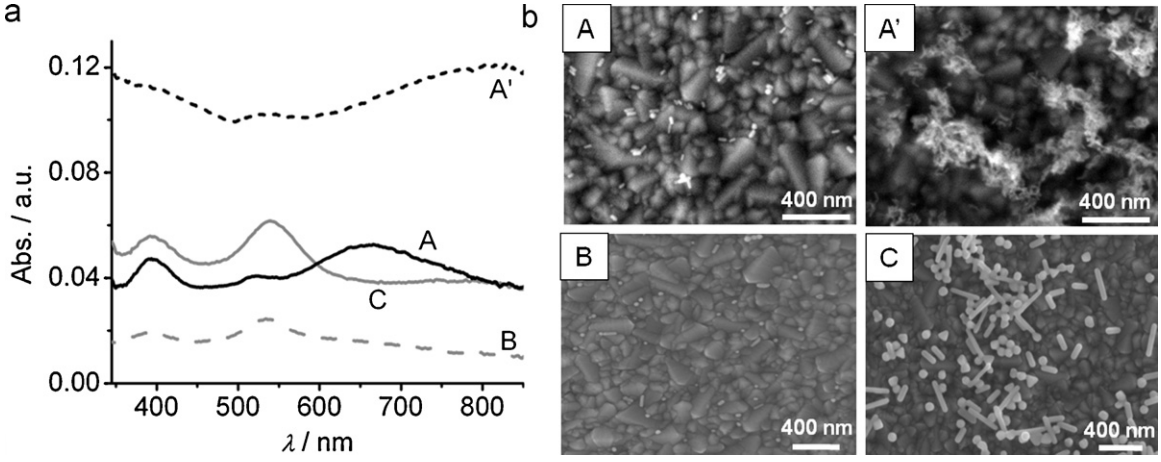

Fig. 5. (a) UV–vis spectra and (b) scanning electronic micrographs of the ITO/Au-NPs modified surfaces with Au-NPs from (A) sample A, (A′) sample A′, (B) sample B and (C) sample C.

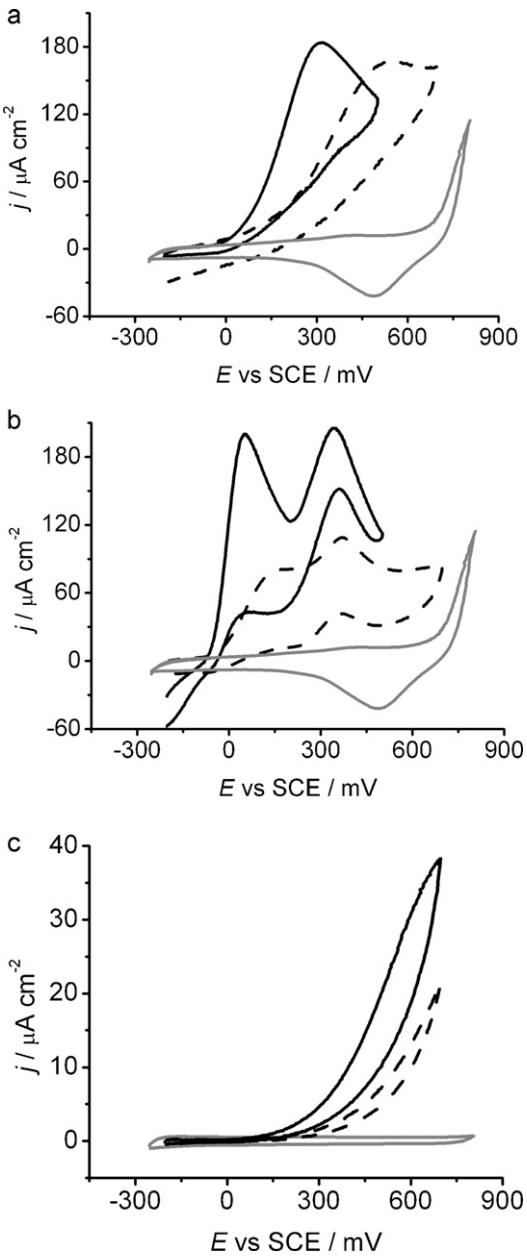

Fig. 6. Cyclic voltammograms of (a) polycrystalline gold, (b) Au(1 1 1) and (c) ITO surfaces, (—) before and (- - -) after immersion in 0.01 mol dm^{-3} CTAB solution for 18 h, in 0.5 mmol dm^{-3} AA solution in PB 0.1 mol dm^{-3} (pH 7) and (—) comparison with voltammograms in blank solution; $\nu = 50$ mV s^{-1}.

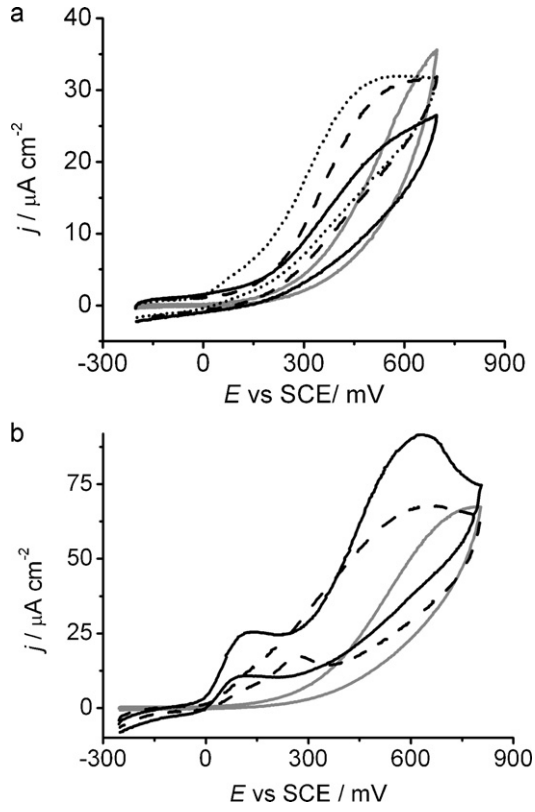

Fig. 7. Cyclic voltammograms obtained for ITO/Au-NPs modified electrodes with nanoparticles from (a) sample A′ (black lines, (—), (- - -) and (·····) in 3 independent experiments), (b) sample B (- - -) and sample C (—) and comparison with bare ITO surface (grey line) in 0.1 mol dm^{-3} PB (pH 7) solution containing 0.5 mmol dm^{-3} AA; $\nu = 50$ mV s^{-1}.

single-crystal surfaces such as the (1 1 1), presented in Fig. 6b, two oxidation waves are observed at 54 and 345 mV.

In order to evaluate the influence of the surfactant, used in the Au-NPs synthesis, on the electrochemical response of the electrodes, Au and ITO surfaces have been immersed in a 0.01 mol dm^{-3} CTAB solution for 18 h and the voltammetric profiles (Fig. 6c) contrasted with those obtained on clean electrodes (Fig. 6a and b). It is clear that CTAB interacts with the bulk gold and ITO surfaces, modifying their electrochemical response; the oxidation process shifts to higher potential values and the oxidation current decreases. However, it is noteworthy that for the (1 1 1) gold surface the single crystalline behaviour prevails and two oxidation waves are detected at c.a. 155 and 370 mV, respectively, after contact with the CTAB solution (Fig. 6b).

Contrarily to the reported potential decrease of the AA anion oxidation, due to the electrostatic attraction to electrode surfaces modified with adsorbed cationic surfactants such as CTAB or DDAB [14,15], it has not been observed since better response was obtained for the clean electrodes.

In spite of some irreproducibility which may be due to difficulties in controlling the amount of immobilised nanoparticles on the ITO surface through the drop-cast method, the voltammetric responses of 3 independent experiments, obtained for the Au-NPs of sample A′, depicted in Fig. 7a, show a polycrystalline-like behaviour, the AA oxidation occurring at higher overpotential than on bulk polycrystalline gold surface. The larger amount of attached Au-NPs and the presence of aggregated particles, revealed by SEM imaging (Fig. 5b), resulted in a weak electrochemical response suggesting poor electric contact between these nanoparticles and the substrate. On the other hand, by using the CTAB-stabilised nanoparticles from samples B and C, a lower overpotential for the AA oxidation reaction than for sample C′ is observed and two AA oxidation processes are detected in the voltammograms shown in Fig. 7b at about 160 and 600 mV, resembling the single-crystal behaviour presented before (Fig. 6b). Nevertheless, insight on the effect of size, shape and surface structure in the electrochemical response of the Au-NPs is hampered due to the broad range detected for these samples and showed in the SEM images (Fig. 5b).

The referred characteristics of the Au-NPs of sample A (homogeneous shape and size and surface domains comprising (1 1 1) and (1 1 0) facets) should allow a better understanding on the surface domains and CTAB influence on the electrochemical behaviour. The data presented in Fig. 8a show that these particles display a single-crystal like response with two AA oxidation waves at about 110 and 440 mV. Moreover, higher oxidation currents and lower overpotentials than for the "surfactant-free" sample are observed. These results confirmed that the interaction of the CTAB with gold facets

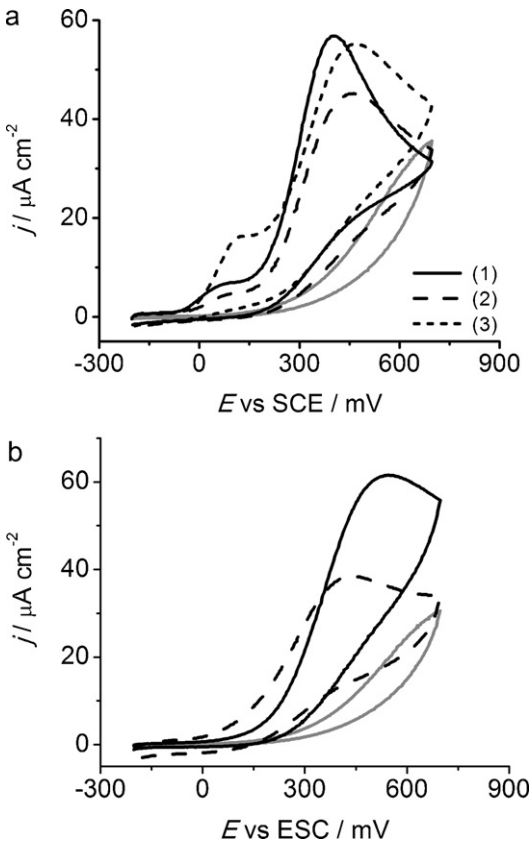

Fig. 8. Cyclic voltammograms obtained for ITO/Au-NPs of (a) sample A modified electrode (black lines, (—), (- - -) and (·····) in 3 independent experiments) and (b) (—) CTAB-stabilised and (- - -) "surfactant-free" cubic Au-NPs and comparison with bare ITO surface (grey line) in 0.1 mol dm^{-3} PB (pH 7) solution containing 0.5 mmol dm^{-3} AA; $\nu = 50$ mV s^{-1}.

in the Au-NPs surface influences their electrochemical response, in agreement to that observed for bulk gold surfaces (Fig. 6a and b). The potential values of the two AA oxidation waves can be correlated to that observed on the Au(1 1 1) surface after contact with the CTAB solution (c.a. 155 and 370 mV). Therefore it is the less strong interaction strength with the (1 1 1) facets, than with the (1 1 0) surface domains, that facilitates the access of the AA to the (1 1 1) surface, Scheme 1. In fact, by using CTAB-stabilised cubic nanoparticles with average size of 42 ± 2 nm prepared according to the procedure reported in the literature [4,10,22], which present faces with (1 0 0) surface domains that are more strongly stabilised by the

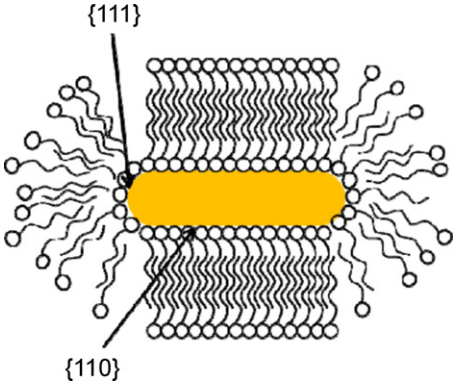

Scheme 1.

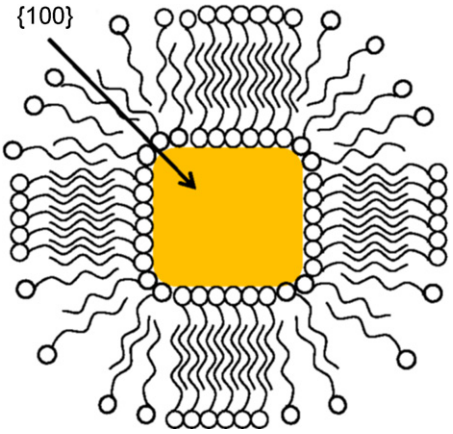

Scheme 2.

surfactant, the single-crystal like behaviour has not been detected, confirming that the stronger interaction of CTAB occurs with the (1 0 0) facets (Fig. 8b) and no other single-crystalline gold surface is available to the AA oxidation reaction. Although the electrochemical response displaying a single oxidation wave in CTAB-stabilised cubic Au-NPs reflect the less organised surfactant bilayer at the edges of cubes (Scheme 2) and concomitant access of the AA to the poly-oriented Au surface, in "surfactant-free" gold nanocubes, it results from the mean crystallographic orientation of the clean surface.

Further support for those statements has been provided by the response collected with an electrode modified with Au-NPs from sample A′ and then immersed in a CTAB solution for c.a. 17 h. The voltammograms displayed in Fig. 9 illustrate the electrochemical responses of the electrode modified with the "surfactant-free" Au-NPs before and after contact with the CTAB solution. In the presence of CTAB the single crystal like profile is re-establish with the two AA oxidation waves occurring at 85 and 300 mV, respectively, close to that detected for the Au(1 1 1) surface and therefore confirming that are the less stabilised Au(1 1 1) surface domains the responsible for the enhanced electrocatalytic performance. It is noteworthy that the hypothesis of poor electric contact between the "surfactant-free" Au-NPs and the substrate has not been verified since after contact with the surfactant solution the two AA oxidation processes are again detected.

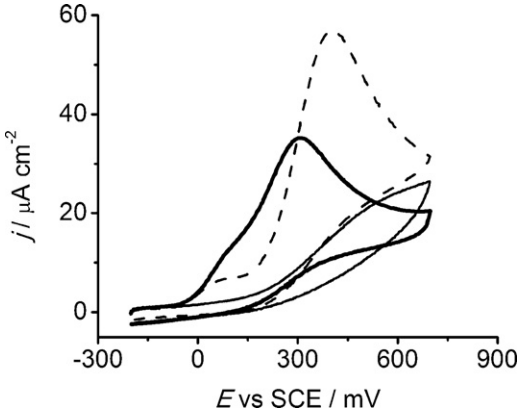

Fig. 9. Cyclic voltammograms obtained for the ITO/Au-NPs sample A′ (thin solid line), ITO/Au-NPs sample A (dash line) and ITO/Au-NPs sample A′ after immersion in CTAB solution for 17 h (thick line), in 0.1 mol dm^{-3} PB (pH 7) solution containing 0.5 mmol dm^{-3} AA; $\nu = 50$ mV s^{-1}.

4. Conclusions

The rigorous control of the synthesis conditions allowed the preparation of rod-shaped Au-NPs with homogeneous size. Using distinct growth conditions, as the absence of silver ions (samples B and C) and addition of sodium hydroxide (sample C) to the growth solution, resulted in polymorphic and heterogeneously sized particles, as confirmed by TEM imaging. The average surface of the prepared Au-NPs showed high contribution from the (1 1 1) facet in the XRD analysis, whereas for the rod-shaped Au-NPs it was possible to identify the presence of both (1 1 1) and (1 1 0) surface domains by lead UPD, in agreement with the reported in the literature for these particles.

The AA oxidation reaction, used for the evaluation of the electrochemical properties of the synthesised Au-NPs, revealed to be sensitive to the electrode nature (polycrystalline or single-crystal surface) and the electrochemical response was influenced by the presence of CTAB. Indeed, the CTAB interacts with the ITO and gold surfaces but contrary to that reported in the literature, the electrochemical response towards the AA oxidation was hampered.

On the rod shaped Au-NPs, comprising (1 1 1) and (1 1 0) facets, the (1 1 0) surface domains are preferentially stabilised by the CTAB while the (1 1 1) facets persist available for the AA oxidation reaction, which results in a single crystal like electrochemical behaviour. On the other hand, for the corresponding "surfactant-free" Au-NPs, improvement of the electrochemical response has not been observed owing to the contribution of the average surface i.e., the (1 1 1) and (1 1 0) surface domains and their boundaries. For the cubic Au-NPs the observed electrochemical polycrystalline like behaviour is due to the strong interaction of the CTAB with the (1 0 0) facets exposing the poly-oriented cube edges, and the contribution of the "surfactant-free" nanocubes.

The dissimilar interaction of CTAB with the gold surface domains (stronger with the (1 1 0) facets than with the (1 1 1) surface domains) enables the discrimination of surface crystallographic orientation contribution to the electrocatalytic performance of the Au-NPs. The exposed (1 1 1) crystallographic facets are the responsible for the CTAB-stabilised rod shaped Au-NPs reactivity towards the surface sensitive reaction under study.

Acknowledgement

V.C. Ferreira gratefully acknowledge the financial support from Fundação para a Ciência e a Tecnologia, scholarships SFRH/BD/30585/2006.

References

[1] T.K. Sau, C.J. Murphy, Langmuir 20 (2004) 6414.
[2] D. Seo, J.C. Park, H. Song, J. Am. Chem. Soc. 128 (2006) 14863.
[3] Y. Chen, W. Schuhmann, A.W. Hassel, Electrochem. Commun. 11 (2009) 2036.
[4] J. Hernández, J. Solla-Gullón, E. Herrero, A. Aldaz, J.M. Feliu, J. Phys. Chem. C 111 (2007) 14078.
[5] N. Malikova, I. Pastoriza-Santos, M. Schierhorn, N.A. Kotov, L.M. Liz-Marzán, Langmuir 18 (2002) 3694.
[6] F.J. Vidal-Iglesias, J. Solla-Gullón, P. Rodríguez, E. Herrero, V. Montiel, J.M. Feliu, A. Aldaz, Electrochem. Commun. 6 (2004) 1080.
[7] J. Hernández, J. Solla-Gullón, E. Herrero, A. Aldaz, J.M. Feliu, J. Phys. Chem. B 109 (2005) 12651.
[8] J. Hernández, J. Solla-Gullón, E. Herrero, A. Aldaz, J.M. Feliu, Electrochim. Acta 52 (2006) 1662.
[9] J. Hernández, J. Solla-Gullón, E. Herrero, J. Electroanal. Chem. 574 (2004) 185.
[10] J. Hernández, J. Solla-Gullón, E. Herrero, J.M. Feliu, A. Aldaz, J. Nanosci. Nanotechnol. 9 (2009) 2256.
[11] J. Solla-Gullón, P. Rodríguez, E. Herrero, A. Aldaz, J.M. Feliu, Phys. Chem. Chem. Phys. 10 (2008) 1359.
[12] J. Pérez-Juste, I. Pastoriza-Santos, L.M. Liz-Marzán, P. Mulvaney, Coord. Chem. Rev. 249 (2005) 1870.
[13] C.J. Johnson, E. Dujardin, S.A. Davis, C.J. Murphy, S. Mann, J. Mater. Chem. 12 (2002) 1765.
[14] S.-M. Chen, W.-Y. Chzo, J. Electroanal. Chem. 587 (2006) 226.
[15] R. Hosseinzadeh, R.E. Sabzi, K. Ghasemlu, Colloids Surf. B 68 (2009) 213.
[16] J. Zhang, M. Kambayashi, M. Oyama, Electrochem. Commun. 6 (2004) 683.
[17] A. Sivanesan, P. Kannan, S.A. John, Electrochim. Acta 52 (2007) 8118.
[18] V.C. Ferreira, A.M. Melato, A.F. Silva, L.M. Abrantes, Electrochim. Acta (2011) doi:10.1016/j.electacta.2010.11.033.
[19] G.-Z. Hu, D.-P. Zhang, W.-L. Wu, Z.-S. Yang, Colloids Surf. B 62 (2008) 199.
[20] R.N. Goyal, A. Aliumar, M. Oyama, J. Electroanal. Chem. 631 (2009) 58.
[21] B.K. Jena, C.R. Raj, Electrochem. Commun. 10 (2008) 951.
[22] C.M. Sánchez-Sánchez, F.J. Vidal-Iglesias, J. Solla-Gullón, V. Montiel, A. Aldaz, J.M. Feliu, E. Herrero, Electrochim. Acta 55 (2010) 8252.
[23] B.D. Busbee, S.O. Obare, C.J. Murphy, Adv. Mater. 15 (2003) 414.
[24] K. Kwon, K.Y. Lee, Y.W. Lee, M. Kim, J. Heo, S.J. Ahn, S.W. Han, J. Phys. Chem. C 111 (2007) 1161.
[25] X.C. Jiang, M.P. Pileni, Colloids Surf. A 295 (2007) 228.
[26] J. Yang, J.Y. Lee, H.-P. Too, Anal. Chim. Acta 546 (2005) 133.
[27] P.L. Gai, M.A. Harmer, Nano Lett. 2 (2002) 771.
[28] B. Ballarin, M.C. Cassani, E. Scavetta, D. Tonelli, Electrochim. Acta 53 (2008) 8034.
[29] O.P. Khatri, K. Murase, H. Sugimura, Langmuir 24 (2008) 3787.
[30] X. Xing, M. Shao, M.W. Hsiao, R.R. Adzic, C.-C. Liu, J. Electroanal. Chem. 339 (1992) 211.
[31] M. Rueda, A. Aldaz, F. Sanchez-Burgos, Electrochim. Acta 23 (1978) 419.
[32] M.I. Manzanares, V. Solís, R.H. Rossi, J. Electroanal. Chem. 407 (1996) 141.